Microfabricated atomic frequency references

J Kitching[1]**, S Knappe**[1]**, L Liew**[2]**, J Moreland**[2]**, P D D Schwindt**[1]**,
V Shah**[3]**, V Gerginov**[4] **and L Hollberg**[1]

[1] Time and Frequency Division, The National Institute of Standards and Technology,
Boulder, CO 80305, USA
[2] Electromagnetics Division, The National Institute of Standards and Technology, Boulder,
CO 80305, USA
[3] Department of Physics, The University of Colorado, Boulder, CO 80309, USA
[4] Department of Physics, The University of Notre Dame, South Bend, IN 46556, USA

Abstract

Using microfabrication processes, we have been able to construct physics
packages for vapour cell atomic frequency references $100\times$ smaller than
previously existing versions, with a corresponding reduction in power
consumption. In addition, the devices offer the potential for wafer-level
fabrication and assembly, which would substantially reduce manufacturing
costs. It is anticipated that a complete frequency reference could be
constructed based on these physics packages with a total volume below
$1\,cm^3$, a power dissipation near $30\,mW$ and a fractional frequency instability
below 10^{-11} over time periods from hours to days. Such a device would
enable the use of atomically precise timing in applications that require
battery operation and portability, such as hand-held global positioning
system receivers and wireless communication systems.

1. Introduction

The simplest and most easily implemented atomic frequency
references are based on microwave transitions in atoms
confined in a vapour cell at room temperature. While more
advanced methods of confining and controlling atoms (such
as the use of atomic beams, and laser cooling and trapping
with electromagnetic fields) allow longer atomic coherence
lifetimes and hence better performance, atomic clocks based
on vapour cells continue to be widely used in a variety of
applications.

It was recognized early on that atomic clocks would
probably have a considerable impact on communications
industries and military services. This impact is still being
felt today, as atomic frequency references with volumes near
$100\,cm^3$ are being manufactured by the tens of thousands for
installation in modern cellular telephone networks [1]. Low-
power, space-qualified atomic clocks also form the core of the
global positioning system (GPS), which is rapidly becoming a
critical part of the world's technological infrastructure. Even
smaller, lower-power frequency references installed in GPS
receivers could enable direct acquisition of the military P(Y)
GPS code and hence enhance the resistance of the receiver to
jamming [2, 3]. In part, the importance of compact vapour cell
atomic frequency references to modern applications such as
network synchronization has been due to engineering advances
that have allowed a high degree of miniaturization, and
associated reductions in manufacturing cost, power dissipation
and improvements in reliability. It is this perspective that has
motivated recent work at The National Institute of Standards
and Technology (NIST) and some other laboratories to develop
highly miniaturized, low-power atomic frequency references
based on micromachining techniques.

The use of micromachining, based on photolithography
and selective etching, allows enormous reductions in the
size and power dissipation of atomic frequency reference
physics packages, as compared with previously developed
devices [4]. The size reduction is a result of the small feature
dimensions and highly scalable nature of the photolithographic
micromachining process. Highly compact atomic vapour
cells in turn result in lower power dissipation since better
thermal isolation from the environment can be achieved with
thinner support structures and a smaller radiating surface area.
Finally, multiple structures can be fabricated in parallel by
simply reproducing the etch mask across the wafer. This
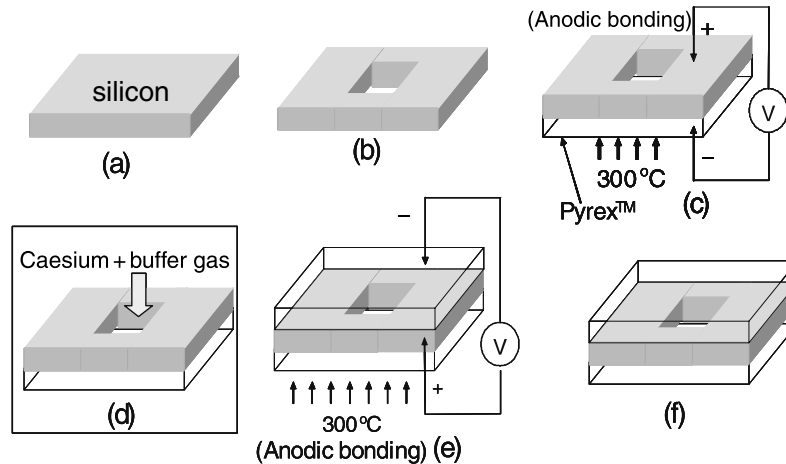aspect opens the door to reduced cost. Several key steps

Figure 1. Schematic showing the steps in wafer-level fabrication of an alkali cell.

in the development of microfabricated frequency references have been accomplished to date in our laboratory including an estimate of the performance as a function of cell size [5], the development of microfabricated alkali atom vapour cells [6, 7] and the integration of those cells into a compact physics package assembly [8, 9].

2. Microfabricated atomic vapour cells

At the heart of our atomic frequency references are alkali atom vapour cells fabricated [6, 7] with techniques usually applied to microelectromechanical systems (MEMS). The cells are formed by sandwiching a silicon wafer, with one or more holes etched through it, between two transparent glass wafers, as shown in figure 1. Typically, the interior volume of the cells is about 0.5 mm^3. However, the scalable nature of the etching process would allow cell volumes as small as 10^{-6} mm^3 to be fabricated simply by changing the etch mask and wafer thickness. We have demonstrated cells with characteristic lengths between 200 μm and several millimetres.

The cell windows are attached to the surface of the silicon by the use of anodic or field-assisted bonding [10]. Alkali atoms are confined in the cell by depositing a mixture of BaN$_6$ and CsCl into the cell before the final window is bonded. The sample is then heated to 150 °C inside a vacuum chamber, at which point the chemicals react and create Cs, BaCl and N$_2$. The chamber is then backfilled with an appropriate buffer gas. The final window is then pushed up against the top of the sample, and the cell is heated further with an electric field applied to seal the Cs and the buffer gas inside the cell (figure 1(e)). The residual N$_2$ gas produced by the reaction is pumped or diffuses away before the cell is sealed, since the final buffer-gas pressure in the cell roughly matches the pressure in the chamber during bonding.

After the final bonding step, the cells can be diced into individual components. A cell fabricated by the use of the first method described above is shown in figure 2. We believe that the process outlined in figure 1 could be easily implemented at the wafer level. Lithographic patterning, etching and bonding of entire wafers are routinely done in the MEMS field, and cells could be filled by simultaneous deposition of a chemical solution (chemical reaction technique). We have been able to
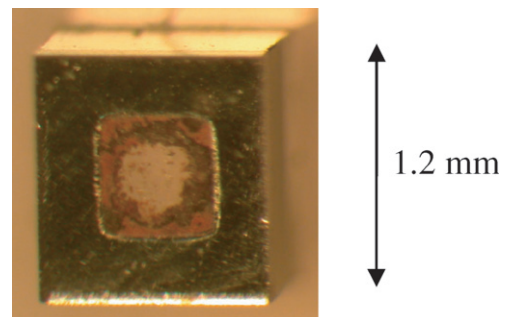

Figure 2. Photograph of a micromachined Cs vapour cell fabricated by anodic bonding.

(This figure is in colour only in the electronic version)

fabricate eight cells simultaneously with a vacuum system of modest size and complexity.

3. Physics package assembly

The physics package architecture is based on the excitation of coherent population trapping (CPT) resonances [11] in the atoms with a frequency-modulated diode laser [12]. This excitation method has the advantage over the more conventional microwave excitation in that it is simpler to implement and does not require the use of a microwave cavity, which can limit the size reduction. The laser is modulated at a frequency close to one-half the atomic hyperfine splitting; the modulation creates two first-order sidebands separated by a frequency equal to the hyperfine splitting. These two sidebands excite a coherence in the atoms between the magnetically-insensitive Zeeman components of each hyperfine level. The absorption of light by the atomic sample is altered by the coherence, and the change is detected by monitoring the transmitted laser power.

Most of the chip-scale atomic frequency references assembled at NIST over the last year have a very similar structure, illustrated in figure 3 [8]. A die containing a vertical-cavity surface-emitting laser (VCSEL) is bonded onto a substrate patterned with gold (figure 3(A), layer a). The VCSEL is used because of its low power requirements
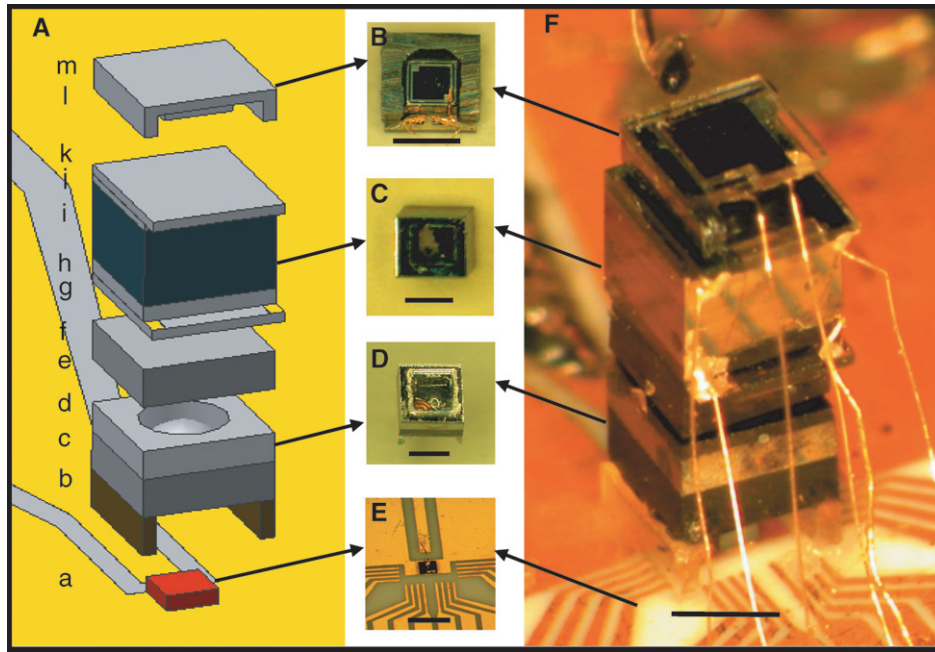
Figure 3. The microfabricated atomic clock physics package based on Cs atoms. (A) Schematic of assembly. Layers from bottom to top: a, laser and baseplate; b, glass; c, ND filter; d, spacer; e, quartz (not shown); f, ND filter; g, glass/ITO; h, glass; i, Si; j, glass; k, glass/ITO; l, Si; m, glass. Total height, 4.2 mm; width and depth, 1.5 mm. Photographs (B), photodiode assembly; (C), cell assembly; (D), optics assembly; (E), laser assembly; (F), the full atomic clock physics package realized as a microchip. The black lines in the photographs indicate 1 mm.

(This figure is in colour only in the electronic version)

(typically <5 mW for most devices), high modulation efficiency and availability of single-mode devices at the 852 nm optical transition in Cs and the 780 nm and 795 nm optical transitions in ^{87}Rb.

The light emitted by the VCSEL (figure 3(E)) is conditioned by an optics assembly (figure 3(A), layers b–f; figure 3(D)) attached to the baseplate. This optics assembly attenuates and collimates the light and changes the light polarization from linear to circular. In this vertically integrated structure, glass spacers (figure 3(A), layer b) support the rest of the device assembly over the laser and provide thermal isolation between the heated cell and the baseplate. Two neutral-density filters (figure 3(A), layers c and f), cut from a wafer of optically dense glass, attenuate the light power to roughly 10 μW and the light is collimated by means of a commercially available microrefractive lens fabricated by inkjet deposition of optical epoxy (figure 3(A), layer d). The light polarization is altered with a piece of a quartz wafer, 80 μm thick, with its optical axis oriented at 45° to the direction of the initial polarization of the laser beam (figure 3(A), layer e, not shown).

The cell assembly (figure 3(A), layers g–k; figure 3(C)) is placed on top of the optics assembly. During operation of the frequency reference, the cell is heated with planar heaters (figure 3(A), layers g and k), fabricated from a thin layer of transparent indium-tin oxide (ITO) deposited on a glass substrate and then wire-bonded to the substrate through gold contact strips. Heaters are placed above and below the cell to provide uniform heating when a current is passed through the ITO film. Because the heat enters the cell though the windows, these parts remain slightly warmer than the cell body, which prevents build-up of an opaque alkali metal film on the windows that might prevent light from entering or exiting the cell. Finally, a photodiode assembly (figure 3(A), layers l–m and figure 3(B)) is mounted onto the top of the structure to detect the light power transmitted through the cell.

In most cases, the layers are bonded together with optical epoxy. Gold wires with diameter 25 μm are bonded on one end to individual components before they are assembled and their other ends are bonded to the baseplate after assembly. We anticipate that with further refinement of the design, all wires can be bonded after assembly of the entire structure. Photographs of the fully assembled device and individual components are shown in figure 3(B)–(F).

4. Device characterization

The first physics package characterized at NIST was based on Cs and operated with the temperature of the alkali vapour cell at about 80 °C. Modulation at 4.6 GHz, one-half of the Cs ground-state hyperfine oscillation frequency, was applied to the laser. The change in the dc transmitted optical power was monitored with the photodiode at the top of the structure. A plot of the photodiode signal as a function of the detuning of twice the modulation frequency is shown in figure 4.

The local oscillator (LO) is stabilized onto the atomic resonance with phase-sensitive detection. The stabilized output frequency of the LO is then compared to a secondary, more stable oscillator to measure its frequency as a function of time. When integrated for a period τ, the fractional frequency instability as measured by the Allan deviation is shown in figure 5. A frequency instability of 2.5×10^{-10} at 1 s of
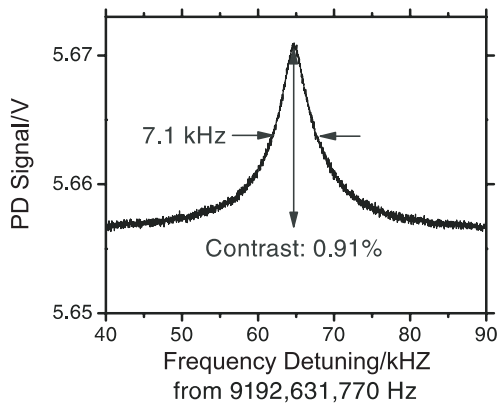
Figure 4. CPT resonance signal from the microfabricated atomic clock physics package shown in figure 3. The resonance linewidth is 7.1 kHz.
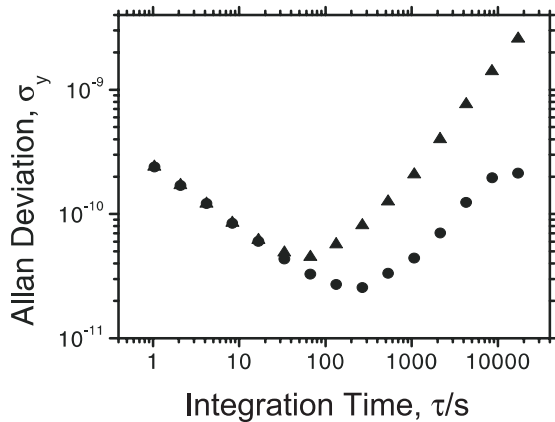

Figure 5. Fractional frequency instability of the microfabricated atomic frequency reference as a function of integration time. Triangles indicate the stability as-measured and circles indicate the stability after removal of the linear frequency drift.

integration is obtained, which reaches a noise floor of 4×10^{-11} near 100 s. A linear frequency drift of -1.6×10^{-8}/day is also observed, which we attribute to chemical reactions occurring in the cell that change the pressure of the buffer gas and, therefore, also the frequency of the clock. This drift can be reduced substantially by fabricating cells that do not contain Ba [13].

Atomic frequency references based on highly miniaturized vapour cells suffer a fundamental degradation in short-term frequency stability when compared with frequency references based on larger cells because of the more frequent interaction of the alkali atoms with the cell walls [5]. This interaction decreases the atomic coherence time, and therefore lowers the Q-factor of the atomic resonance. One can partially compensate for the effects of this increased wall collision rate by increasing the pressure of the buffer gas contained in the cell, which slows the diffusion of the alkali atoms to the cell walls. However, at very high buffer-gas pressures, collisions of alkali atoms with the buffer-gas atoms dominate the decoherence rate and the clock performance is again degraded.

In the frequency reference described here, wall collisions and optical power broadening are the primary sources of broadening of the linewidth of the microwave transition; spin-exchange broadening and pressure broadening provide

additional small contributions. The noise is dominated by shot noise in the conversion of optical power into electrons in the photodiode, with other contributions due to the conversion of laser FM noise into AM noise by the atomic absorption profile and noise in the detection electronics [14]. The short-term instability can be reduced by exciting the CPT resonance using light resonant with the D1 transition [9, 15], which creates a larger resonance amplitude and therefore increases the signal-to-noise ratio.

The long-term instability of the physics package shown in figure 3 is dominated by the drift described above. Additional effects found to be important with regard to long-term stability are changes in the cell temperature, which affect the device output frequency through the pressure shift, and changes in the laser power and sideband structure, which affect the output frequency through the ac Stark shift.

A total of five physics packages was assembled at NIST within a year of the operation of the first. These were assembled by hand, largely from individually fabricated subsystems, and manually wire-bonded to the substrate. However, the structure is highly compatible with standard wafer-level microfabrication processes and we anticipate that large-scale parallel fabrication of devices would be possible without a fundamental change in the structural design.

5. Power dissipation

The electrical power required to run the physics package was 73 mW, and was dominated by the power required to heat the cell above the ambient temperature of 46 °C set by the baseplate. Independent temperature control of the laser was not implemented in the design described here and the high baseplate temperature (46 °C) was required to tune the particular laser used in the device to the correct wavelength.

By modelling the heat flow in the structure, both analytically and with a finite-element computation, the heat loss channels could be roughly identified. We estimate that 30 mW is lost to conduction through the lower spacer unit, and that 24 mW is lost to conduction through the six gold wire-bonds providing the electrical connections to the baseplate. The remainder is presumably lost to radiation and to conduction to the air surrounding the physics package. Our modelling suggests that these last two heat-loss channels could be reduced to well below 1 mW by the use of vacuum packaging with a low-emissivity coating on its interior surface. The remaining sources of heat loss, conduction through the lower spacer unit and the wire-bonds, can be addressed through more advanced thermal design of the spacer unit itself. Analytical and finite-element modelling, for example, show that the use of a polymer material with a lower thermal conductivity and thin (10 μm) gold traces as part of the electrical path would reduce the heater power to below 12 mW to maintain a temperature difference of 50 K between the baseplate and the cell [16].

6. Integrated system

In addition to the physics package, two other components are required to form a complete atomic frequency reference. The development of small low-power oscillators at gigahertz frequencies with sufficient frequency stability to be able to be

locked to the atomic resonance is being undertaken by a number of research groups. In addition, a digital control system based on a microprocessor is being developed at NIST and is expected to be able to implement the four feedback loops (two temperature control loops, two lock-in detectors) necessary to run the frequency reference using under 10 mW of electrical power. After miniaturization of the control electronics in an application-specific integrated circuit (ASIC) and integration with the physics package described above and a compact LO, we expect that the volume of the complete frequency reference could be near 1 cm^3. The anticipated power dissipated by such a device is roughly 30 mW, divided roughly equally between physics package, LO and control electronics.

7. Conclusion

The field of precision timing is now experiencing the revolutionary impact that MEMS has had in a wide range of other areas, from chemical detection to power sources. It seems likely that atomic frequency references based on MEMS fabrication techniques will become commercial products in the near future [17]. Commercialization will undoubtedly result in significant improvements in design and performance, leading to smaller, lower-power and less costly devices. In turn, new applications will emerge that are not even on the horizon today. The work described in this paper represents just the first few steps in this direction and many important challenges remain to be overcome. However, the prospects for widespread use of chip-scale atomic clocks are becoming increasingly promising as the development of these devices continues.

Acknowledgments

References

[1] Kusters J A and Adams C A 1999 Performance requirements of communication base station time standards *RF Des.* **22** 28–38

[2] Filler R L and Esposti R D 1998 Clock performance and direct GPS P(Y)-code (re)acquisition *Proc. 52nd IEEE Int. Freq. Control Symp. (Pasdena, CA)* pp 315–9

[3] Fruehoff H 2001 Fast direct-P(Y) GPS signal acquisition using a special portable clock *Proc. 33rd Ann. Precise Time and Time Interval Meeting (Long Beach, CA)* pp 359–69

[4] Chantry P J, Liberman I, Verbanets W R, Petronio C F, Cather R L and Partlow W D 1996 Miniature laser-pumped cesium cell atomic clock oscillator *Proc. 50th IEEE Int. Freq. Control Symp. (Honolulu, HI)* pp 1002–10

[5] Kitching J, Knappe S and Hollberg L 2002 Miniature vapor-cell atomic-frequency references *Appl. Phys. Lett.* **81** 553–5

[6] Liew L, Knappe S, Moreland J, Robinson H G, Hollberg L and Kitching J 2004 Micromachined alkali atom vapor cells *Appl. Phys. Lett.* **84** 2694–6

[7] Liew L-A, Knappe S, Moreland J, Robinson H, Hollberg L and Kitching J 2004 Micromachined alkali atom vapor cells for chip-scale atomic clocks *Proc. 17th IEEE Int. Conf. Micro Electron Mech. Syst. (Amsterdam)* pp 113–6

[8] Knappe S, Liew L, Shah V, Schwindt P, Moreland J, Hollberg L and Kitching J 2004 A micromachined atomic clock *Appl. Phys. Lett.* **85** 1460–2

[9] Knappe S, Schwindt P, Shah V, Hollberg L, Kitching J, Liew L and Moreland J 2004 A chip-scale atomic clock based on ^{87}Rb with improved frequency stability *Opt. Express* **13** 1249–53

[10] Wallis G and Pomerantz D I 1969 Field assisted glass-metal sealing *J. Appl. Phys.* **40** 3946–9

[11] Arimondo E 1996 Coherent population trapping in laser spectroscopy *Prog. Opt.* **35** 257–354

[12] Kitching J, Hollberg L, Knappe S and Wynands R 2001 Compact atomic clock based on coherent population trapping *Electron. Lett.* **37** 1449–51

[13] Knappe S, Schwindt P D D, Gerginov V, Shah V, Hollberg L, Kitching J, Liew L and Moreland J 2004 *Proc. 36th Ann. Precise Time and Time Interval Syst. App. Meeting (Washington, DC)* at press

[14] Kitching J, Knappe S, Vukicevic N, Hollberg L, Wynands R and Weidmann W 2000 A microwave frequency reference based on VCSEL-driven dark line resonances in Cs vapor *IEEE Trans. Instrum. Meas.* **49** 1313–7

[15] Stahler M, Wynands R, Knappe S, Kitching J, Hollberg L, Taichenachev A and Yudin V 2002 Coherent population trapping resonances in thermal Rb-85 vapor: D-1 versus D-2 line excitation *Opt. Lett.* **27** 1472–4

[16] Kitching J, Knappe S, Schwindt P D D, Shah V, Liew L and Moreland J 2004 Power dissipation in a vertically integrated chip-scale atomic clock *Proc. 58th IEEE Int. Freq. Control Symp. (Montreal)* at press

[17] See, for example, the work described in Lutwak R *et al* 2004 The chip-scale atomic clock—low-power physics package *Proc. 36th Ann. Precise Time and Time Interval Syst. App. Meeting (Washington, DC)* at press